Bulletin of the JSME Vol.1, No.2, 2014
Mechanical Engineering Reviews

# Deviational methods for small-scale phonon transport

Jean-Philippe M. PÉRAUD*, Colin D. LANDON* and Nicolas G. HADJICONSTANTINOU*
*Department of Mechanical Engineering, Massachusetts Institute of Technology
Cambridge, MA 02139, USA
E-mail: ngh@mit.edu

**Received 13 May 2014**

**Abstract**
We review deviational methods for solving the Boltzmann equation governing phonon transport processes in the context of small-scale, solid-state heat transfer. We briefly discuss the numerical foundations of deviational algorithms as well as basic simulation methodology. Particular emphasis is given to recent developments in the field yielding appreciable efficiency improvements, such as linearized and adjoint formulations, and their applications to complex multiscale problems. Recently developed methods for simulating the ab initio collision operator for applications to phonon transport in novel two-dimensional materials, such as graphene, are also reviewed and discussed.

***Key words*** : Nanoscale heat transfer, Monte carlo, Boltzmann equation, Simulation

## 1. Introduction

Deviational methods are a class of stochastic particle simulation tools for solving kinetic equations. They have been developed [1–3] to alleviate the most important, perhaps, disadvantage of MC methods, namely their inability to efficiently simulate low-signal problems, such as small temperature differences. Deviational methods reduce statistical uncertainty by making use of deterministic information, a technique widely known as control-variate variance reduction [4]. In the case of kinetic equations, deviational methods make use of the observation that statistical noise becomes a limitation when transport signals are small, that is, the system state is close to equilibrium. By using that equilibrium state as a control, and using a stochastic method to simulate the deviation therefrom, deviational methods leverage exact solutions and focus the computational resources onto the unknown component of the phonon distribution function. As discussed further in Section 8, the ability to focus computational resources on the non-equilibrium component of the distribution function is very valuable for simulating multiscale problems.

In the context of small-scale processes, the need for solving kinetic equations such as the Boltzmann transport equation (BTE), arises from the fact that the more tractable continuum description is only a limiting description valid in the limit of "small" mean free path, where transport is diffusive. Deviation from diffusive transport can be quantified by the Knudsen number,

$$Kn = \frac{\Lambda}{L},$$

Paper No.14-00243
[DOI: 10.1299/mer.2014fe0013]

where $\Lambda$ denotes the mean free path and $L$ the characteristic transport length scale. Diffusive transport is expected for $Kn \ll 1$; this regime is typically referred to as the continuum regime. When the mean free path is much larger than the system length scale ($Kn \gg 1$), scattering can be neglected and transport can be approximated as ballistic. Between these two limiting cases, that is, when the mean free path is on the same order as the system length scale ($0.1 \lesssim Kn \lesssim 10$), transport is neither diffusive nor ballistic and is referred to as transitional.

The most well known, perhaps, example of such behavior is the breakdown of Navier-Stokes theory, extensively studied in the context of rarefied gas dynamics. In addition to applications related to high altitude aerodynamics, transitional transport has more recently been studied in the context of micro and submicrometer gas dynamics [5] (the mean free path of air molecules at STP is approximately 60nm). A new class of problems that is currently receiving considerable attention is heat transport in semiconducting materials. In these materials, heat is carried by lattice vibrations whose quantized unit is the phonon. With typical semiconductor feature sizes ranging from the nanometer to the millimeter scale [6], phonon transport modeling using a mesoscopic approach such as the BTE is very desirable. Practical applications of interest include the calculation of the thermal conductivity of bulk and nanostructured semiconductors [7–16], fundamental understanding and manipulation of the thermal properties of semiconducting [17–19], as well as low-dimensional materials like graphene [20–22] and solution of coupled electron-phonon transport problems [23–28].

Monte Carlo methods for solving the Boltzmann equation in the context of phonon transport have been recently reviewed by the authors [29]. As a result, this article will only briefly review the basics of deviational simulation and instead focus on recent developments. More details on standard as well as deviational Monte Carlo simulation methods for phonon transport can be found in [29].

## 2. Background

### 2.1 Boltzmann equation for phonon transport

Provided coherence effects can be neglected [14, 30–32], phonon transport is governed by the Boltzmann equation

$$\frac{\partial f}{\partial t} + \nabla_{\mathbf{k}}\omega(\mathbf{k},p)\cdot\nabla_{\mathbf{x}} f = \left[\frac{\partial f}{\partial t}\right]_{\text{scatt}}, \tag{1}$$

where $f = f(t,\mathbf{x},\omega,\theta,\phi,p)$ is the phonon distribution function, $\mathbf{x}$ denotes position vector in physical space, and $\mathbf{k}$ is the wavevector in reciprocal space with magnitude $k$ and direction given by the angles $\theta$, and $\phi$. The phonon frequency $\omega$ is a function of the wavevector through the dispersion relation $\omega(\mathbf{k},p)$; here, $p$ denotes the polarization.

[DOI: 10.1299/mer.2014fe0013]

The scattering operator can be written as [33, 34]

$$\begin{aligned}\left[\frac{\partial f}{\partial t}\right]_{\text{scatt}} = & \sum_{\mathbf{k}',p'} \left\{ f_{\mathbf{k}'p'}(f_{\mathbf{k}p}+1) - f_{\mathbf{k}p}(f_{\mathbf{k}'p'}+1) \right\} \mathcal{Q}_{\mathbf{k}p}^{\mathbf{k}'p'} \\ & + \sum_{\mathbf{k}'p',\mathbf{k}''p''} \left\{ (f_{\mathbf{k}p}+1)(f_{\mathbf{k}'p'}+1) f_{\mathbf{k}''p''} - f_{\mathbf{k}p} f_{\mathbf{k}'p'} (f_{\mathbf{k}''p''}+1) \right\} \mathcal{Q}_{\mathbf{k}p,\mathbf{k}'p'}^{\mathbf{k}''p''} \\ & + \frac{1}{2} \sum_{\mathbf{k}'p',\mathbf{k}''p''} \left\{ (f_{\mathbf{k}p}+1) f_{\mathbf{k}'p'} f_{\mathbf{k}''p''} - f_{\mathbf{k}p} (f_{\mathbf{k}'p'}+1)(f_{\mathbf{k}''p''}+1) \right\} \mathcal{Q}_{\mathbf{k}p}^{\mathbf{k}'p',\mathbf{k}''p''}, \end{aligned} \tag{2}$$

where $\mathcal{Q}$ is the transition rate matrix, determined by the Hamiltonian of interaction and the appropriate conservation laws [34]. The first term in this expression represents "two-phonon" scattering processes, modeling phonon scattering by impurities. The second and third terms correspond to three-phonon (phonon-phonon) scattering; more specifically, the second term corresponds to type I processes in which two phonons combine to create a third phonon, while the third term corresponds to type II processes, in which a single phonon decays into two phonons. Three phonon processes are separated into normal processes, which conserve momentum, and umklapp processes for which

$$\mathbf{k} \pm \mathbf{k}' = \mathbf{k}'' + \mathbf{G} \quad \text{(type I/II processes)}, \tag{3}$$

where $\mathbf{G}$ is a reciprocal lattice vector. Four phonon and higher order processes are typically negligible [35].

The equilibrium solution of the Boltzmann equation is the Bose-Einstein distribution

$$f^{\text{eq}}(\omega, T_{\text{eq}}) = \frac{1}{\exp\left(\frac{\hbar\omega}{k_{\text{B}}T_{\text{eq}}}\right) - 1}, \tag{4}$$

which is parametrized by the equilibrium temperature $T_{\text{eq}}$.

Knowledge of the distribution function allows the calculation of a number of physical observables, such as the number of phonons per unit volume

$$n(t, \mathbf{x}) = \sum_p \int\int\int f(t, \mathbf{x}, \omega, \theta, \phi, p) \frac{D(\omega, p)}{4\pi} d\omega d^2\mathbf{\Omega}, \tag{5}$$

where $\mathbf{\Omega}$ denotes the unit vector whose direction is defined by the polar and azimuthal angles $\theta$ and $\phi$, respectively, and $d^2\mathbf{\Omega}$ denotes the differential solid angle element $\sin(\theta) d\theta d\phi$. Here,

$$D(\omega, p) = \frac{k(\omega, p)^2}{2\pi^2 V_g(\omega, p)} \tag{6}$$

is the density of states used for converting integration over wavevector to integration over frequency (assuming three-dimensional, isotropic material) and $V_g(\omega, p)$ is the magnitude of the group velocity given by $\mathbf{V}_g = \nabla_{\mathbf{k}}\omega(\mathbf{k}, p)$. We note that in addition to an

[DOI: 10.1299/mer.2014fe0013]

isotropic material, we also assumed that the system states are closely spaced allowing conversion of the sum over states to an integration.

Following this notation, the energy density is given by

$$U(t,\mathbf{x}) = \sum_p \int \hbar\omega f(t,\mathbf{x},\omega,\mathbf{\Omega},p)\frac{D(\omega,p)}{4\pi}d\omega d^2\mathbf{\Omega}, \tag{7}$$

while the heat flux is given by

$$\mathbf{q}''(t,\mathbf{x}) = \sum_p \int \hbar\omega \mathbf{V}_g f(t,\mathbf{x},\omega,\mathbf{\Omega},p)\frac{D(\omega,p)}{4\pi}d\omega d^2\mathbf{\Omega}. \tag{8}$$

In systems out of equilibrium, the local temperature is usually defined as the temperature parameter of an equilibrium distribution with the same energy density. Determining its value requires (numerical) solution of

$$\sum_p \int \hbar\omega f(t,\mathbf{x},\omega,\mathbf{\Omega},p)\frac{D(\omega,p)}{4\pi}d\omega d^2\mathbf{\Omega} = \sum_p \int \hbar\omega f^{\mathrm{eq}}(\omega,T)D(\omega,p)d\omega, \tag{9}$$

for $T = T(t,\mathbf{x})$.

Our discussion above assumed three dimensional materials; the corresponding relations for two dimensional materials directly follow from the above definitions. Comprehensive reviews of phonon physics and the associated Boltzmann equation can be found in numerous publications (e.g. [14, 33, 36–38]).

### 2.2 Relaxation-time approximation

Due to the complexity associated with the scattering operator (2), solutions of the Boltzmann equation using this operator have appeared only recently. The mainstream approach to date consists of "modeling" (2) using what is known in the literature as the relaxation-time approximation [36, 39]

$$\left[\frac{\partial f}{\partial t}\right]_{\mathrm{scatt}} = -\frac{f - f^{\mathrm{loc}}}{\tau}, \tag{10}$$

which assumes that out-of-equilibrium modes do not interact, but rather decay independently toward the system local equilibrium with a characteristic timescale $\tau$. Clearly, (10) achieves enormous simplification, to the extent that in order to capture some of the complexity of phonon-phonon interactions, the relaxation time typically needs to be taken to depend on the carrier state (e.g. $\tau = \tau(\omega,p,T)$). In this case, the interpretation of the distribution $f^{\mathrm{loc}} = f^{\mathrm{eq}}(\omega,\tilde{T})$ is more complex [15, 39] because if the temperature parameter, $\tilde{T}$, is set to the local temperature, the scattering operator does not satisfy energy conservation. Therefore, and in order for energy conservation to be strictly satisfied, $\tilde{T}$ is determined by the energy conservation statement

$$\int_\omega \sum_p \frac{\hbar\omega D(\omega,p) f^{\mathrm{loc}}(\omega,\tilde{T})}{\tau(\omega,p,T)}d\omega = \int_{\mathbf{\omega}} \sum_p \frac{\hbar\omega D(\omega,p) f}{4\pi\tau(\omega,p,T)}d\omega d^2\mathbf{\Omega}, \tag{11}$$

[DOI: 10.1299/mer.2014fe0013]

and is referred to as the pseudo-temperature.

Despite being rather crude, the relaxation-time approximation has been successful in describing thermal transport in three-dimensional materials, especially when the relaxation time is treated as frequency dependent [18, 40], making it by far the most prevalent scattering model. As a result, simulation methods have also overwhelmingly focused on this model. Our discussion below also focuses on this model; a discussion on the simulation of the ab initio operator (2) can be found in Section 7.

### 2.3 Monte Carlo simulation

Monte Carlo methods for solving the Boltzmann equation originated in the Direct Simulation Monte Carlo (DSMC), originally conceived by Bird [41]. One of the major breakthroughs associated with DSMC is the realization that the Boltzmann equation may be integrated explicitly in time at a timescale that approaches (but remains smaller than) the scattering timescale (as opposed to the atomistic timescale) by splitting the two major physical processes modeled by the Boltzmann equation, namely advection and carrier-carrier scattering. In other words, given a sufficiently small timestep of duration $\Delta t$, time integration may proceed by interleaving a collisionless advection substep which integrates

$$\frac{\partial f}{\partial t} + \mathbf{V}_g \cdot \nabla_{\mathbf{x}} f = 0 \tag{12}$$

by moving particles ballistically, with a scattering substep which integrates

$$\frac{\partial f}{\partial t} = \left[\frac{df}{dt}\right]_{\text{scatt}}. \tag{13}$$

The scattering step updates the distribution function by stochastically simulating the appropriate [15, 42, 43] number of scattering events between carriers within the same spatial cell.

By choosing scattering partners stochastically, this process essentially treats scattering events as spatially homogeneous within each cell and thus introduces a discretization error. Numerical analysis of such algorithms is significantly more advanced in the rarefied gas literature compared to the phonon transport literature, presumably due to the longer history of Monte Carlo methods in the former (originating in Bird's original 1963 paper). In the rarefied gas dynamics literature it has been shown [44] that algorithms of this type converge to solutions of the Boltzmann equation, provided that a sufficiently fine discretization is employed, namely, an appropriately large number of particles is used, while the integration timestep and cell size are chosen appropriately small. The latter two requirements have been put on a more firm footing more recently when it was shown that the discretization error scales quadratically with the cell size and, provided the algorithm is symmetrized in time [45, 46], quadratically in the timestep. The same work also showed that for errors less than a few percent in the transport coefficients, the (smallest) linear dimension of the cell in which scattering events are processed should

[DOI: 10.1299/mer.2014fe0013]

be smaller than the mean free path [42], while the timestep needs to be smaller than the mean free time.

Monte Carlo methods have become the prevalent Boltzmann solution methods for a number of reasons. They offer simplicity and a formulation that relies more on algorithms that intuitively reproduce the physics of the problem of interest rather than numerically solving the partial differential equation governing it. The latter makes them easy to code, debug and extend to include additional physics for which it may be very difficult to write the governing equation. Additional advantages include their ability to handle the high dimensionality associated with the distribution function better than mesh-based techniques which need to discretize and store the distribution function in phase space. Also, the particle formulation employed by Monte Carlo methods is ideal for accurately and *stably* capturing the propagation of traveling discontinuities in the distribution function [47] resulting from the advection operator in the Boltzmann equation. Finally, the particle formulation naturally employs importance sampling which yields superior computational efficiency [2].

As usual in MC simulation, macroscopic properties of interest are related to moments of the distribution function, and can be recovered via sampling. As a result, these properties can only be estimated to within some statistical uncertainty, which is inversely proportional to the square root of the number of *independent* samples. In the field of kinetic transport, the statistical uncertainty in transport properties relative to their actual value can be quite large; this is a result of both large population variances (e.g. see [29,48]) and the fact that, in most applications of current interest [5], deviations from equilibrium are small (e.g. small temperature differences), leading to (relatively) small signals. Because statistical uncertainty diminishes proportionally to the square root of the number of samples, this situation quickly leads to intractable simulations, especially in cases of very small deviation from equilibrium. Deviational methods, discussed next, have been developed for the purpose of alleviating this limitation.

### 2.4 Deviational methods: motivation and an example

The limitations associated with MC methods discussed above arise from the fact that these methods reproduce the complete fluctuation spectrum, albeit modified by the fact that each computational particle represents a number of real physical particles (molecules, phonon bundles—see [48] for a discussion). As a result, close to equilibrium where transport magnitudes (signals) are small, the signal to noise ratio becomes small, since the noise is dominated by the ever-present equilibrium spectrum.

Deviational methods overcome this limitation by removing the statistical noise associated with the equilibrium part of the distribution. This is achieved by employing the method of control variates, in which the Monte Carlo calculation is used to calculate the difference from a nearby solution that is known deterministically (analytically or numerically) and referred to as the control.

The general idea behind control variates can be illustrated by the following example. Consider the random variable $m$ associated with the outcome of rolling a slightly

[DOI: 10.1299/mer.2014fe0013]

biased die and let $p(m)$ denote the probability of the various possible outcomes. More specifically, let

$$p(m) = \begin{cases} 1/6 + \alpha & \text{if } m = 1, 2, 3 \\ 1/6 - \alpha & \text{if } m = 4, 5, 6 \end{cases}, \tag{14}$$

where $\alpha \ll 1/6$. Although this problem is sufficiently simple for calculation of moments of $p(m)$ to be analytically possible, let us consider, as an example that serves to illustrate the rationale for the development of deviational methods, the calculation of the mean $\langle m \rangle$ by Monte Carlo simulation. Such a simulation could be an idealization of an experiment aimed at extracting the unknown value of $\alpha$ for a particular die. The simulation (experiment) proceeds by generating $M$ random variates $m_i$ with the above probabilities and estimating $\langle m \rangle$ using

$$\bar{m} = \frac{1}{M} \sum_{i=1}^{M} m_i. \tag{15}$$

This estimator is expected to approach the correct value $\langle m \rangle = 3.5 - 9\alpha$ as $M \to \infty$. More specifically, from the central limit theorem we expect the standard deviation of $\bar{m} - \langle m \rangle$ to be

$$\sigma_{\bar{m}-\langle m \rangle} = \sqrt{\frac{Var(m)}{M}} = \sqrt{\frac{35/12 - 81\alpha^2}{M}}. \tag{16}$$

Our ability to discern the value of $\alpha$ from the noisy experimental (simulation) data will depend on the relative magnitudes of the signal $9\alpha$ and the uncertainty given by (16). Clearly, in the limit $\alpha \to 0$ this problem becomes challenging because the noise to signal ratio $\sqrt{35/12}/(9\alpha\sqrt{M})$ diverges for fixed $M$, or alternatively, because it requires $M$ to increase proportionally to $\alpha^{-2}$ for the noise to signal ratio to remain constant.

Deviational formulations overcome this problem by removing the fluctuations associated with the known "baseline" solution (control). In the present case, a deviational formulation takes advantage of the fact that the results for an unbiased die are well known $\langle m(\alpha = 0) \rangle = 3.5$ and proceeds to calculate $\bar{m}$ from

$$\bar{m} = 3.5 + 6\alpha \frac{1}{M} \sum_{i=1}^{M} s_i m_i, \tag{17}$$

where

$$s_i = \begin{cases} 1 & \text{if } m = 1, 2, 3 \\ -1 & \text{if } m = 4, 5, 6 \end{cases}. \tag{18}$$

This can be seen by writing

$$\langle m \rangle = 3.5 + \alpha(1 + 2 + 3 - 4 - 5 - 6) = 3.5 + 6\alpha(1 + 2 + 3 - 4 - 5 - 6)\frac{1}{6}, \tag{19}$$

In other words, in the deviational simulation, the various outcomes ($m = 1, ..., 6$) are equiprobable (probability 1/6), but some events have a negative sign, indicating probability "less than" that of the control. Thus, we have mathematically decomposed

[DOI: 10.1299/mer.2014fe0013]

the problem in a manner that does not correspond to a physical experiment we could perform, but which yields enormous computational gains.

It is easy to show that this formulation is now characterized by a statistical uncertainty $\sqrt{465}\alpha/\sqrt{M}$, which leads to a noise to signal ratio (or relative statistical uncertainty) equal to $\sqrt{465}/(9\sqrt{M})$, that is constant and independent of $\alpha$. In other words, the deviational formulation can be used to solve this problem at arbitrarily small $\alpha$, in contrast to the standard MC approach whose cost (relative to the deviational approach) increases as $\alpha^{-2}$ for small $\alpha$. Here we assume that the costs of the two simulations per sample are similar, as can be concluded from the discussion of their formulation.

It is also important to note that the deviational formulation described here does not introduce any approximation. In other words, its considerable computational advantage derives from introducing (exact) deterministic information and not from an approximation of some form. Clearly the computational benefit will depend on the choice of the baseline distribution (control). For example, for values of $\alpha$ such that $35/12 - 81\alpha^2 < \sqrt{465}\alpha$ (but still $\alpha \leq 1/6$), the standard Monte Carlo approach will be more efficient and should be preferred, but even then the deviational approach should be expected to return the correct answer.

We now proceed to discuss how these ideas can be used to accelerate Monte Carlo simulations of the BTE.

## 3. Deviational methods for phonon transport

The control-variate formulation lends itself naturally to MC methods for solving the BTE, because the control can be readily identified as a nearby Bose-Einstein equilibrium distribution $f^{\mathrm{eq}}(\omega, T_{\mathrm{eq}})$. In principle, the choice of $T_{\mathrm{eq}}$ is fairly arbitrary, provided the resulting deviations from $f^{\mathrm{eq}}(\omega, T_{\mathrm{eq}})$ are small; for further discussion see [29]. Here, as is usually the case, we will always take $T_{\mathrm{eq}} \neq T_{\mathrm{eq}}(t)$; a discussion of the consequences associated with taking $T_{\mathrm{eq}} = T_{\mathrm{eq}}(t)$ can be found in [49].

It was recently shown [3] that it is preferable to simulate the energy-based Boltzmann equation

$$\frac{\partial e}{\partial t} + \mathbf{V}_g \cdot \nabla_{\mathbf{x}} e = \frac{e^{\mathrm{loc}} - e}{\tau(\omega, p, T)}, \tag{20}$$

obtained by multiplying the BTE by $\hbar\omega$ and letting $e = \hbar\omega f$ and $e^{\mathrm{loc}} = \hbar\omega f^{\mathrm{loc}}$. The advantage of this formulation is that particle conservation, which can be enforced exactly, guarantees energy conservation, which is highly desirable and could only be achieved approximately in previous methods and only after cumbersome manipulations of the particle distribution.

In a deviational simulation, computational particles simulate the deviation from equilibrium $e^{\mathrm{d}} = e - e^{\mathrm{eq}}_{T_{\mathrm{eq}}}$, by introducing the approximation $D\, e^{\mathrm{d}}/(4\pi) = \mathcal{E}^{\mathrm{d}}_{\mathrm{eff}} \sum_i s_i \delta^3(\mathbf{x} - \mathbf{x}_i)\delta^2(\boldsymbol{\Omega} - \boldsymbol{\Omega_i})\delta(\omega - \omega_i)\delta_{p,p_i}$ where $s_i$ denotes the particle sign, $\mathcal{E}^{\mathrm{d}}_{\mathrm{eff}}$ denotes the amount of *deviational energy* carried by each computational particle and $e^{\mathrm{eq}}_{T_{\mathrm{eq}}} = \hbar\omega f^{\mathrm{eq}}(\omega, T_{\mathrm{eq}})$. The parameter $\mathcal{E}^{\mathrm{d}}_{\mathrm{eff}}$ is chosen such that the competing requirements of low computational cost

[DOI: 10.1299/mer.2014fe0013]

and good statistical resolution are balanced as well as possible; an extensive discussion can be found in [29]. For $T_{\rm eq} \neq T_{\rm eq}(\mathbf{x})$, the dynamics of these particles are governed by the energy-based deviational Boltzmann equation

$$\frac{\partial e^{\rm d}}{\partial t} + \mathbf{V}_g \cdot \nabla_{\mathbf{x}} e^{\rm d} = \frac{(e^{\rm loc} - e^{\rm eq}_{T_{\rm eq}}) - e^{\rm d}}{\tau(\omega, p, T)}. \tag{21}$$

The case $T_{\rm eq} = T_{\rm eq}(\mathbf{x})$ will be discussed further below and in Section 4.

We now provide a brief outline of the simulation method: more details can be found in [3, 29]. The simulation is initialized by sampling the initial deviational distribution $e(t=0) - e^{\rm eq}_{T_{\rm eq}}$, where $e(t=0) = \hbar\omega f(t=0)$ and $f(t=0)$ is the initial condition on the phonon distribution. Time-integration proceeds using a splitting algorithm with timestep $\Delta t$. During advection, particles encountering one of the simulation domains are treated according to the boundary condition corresponding to that boundary. Particles are also generated volumetrically if a spatially variable equilibrium distribution has been chosen (see Section 4). During the collision step, particles to be scattered are chosen based on their respective frequency-dependent scattering rate

$$\frac{\Delta t}{\tau(\omega, p, T)}. \tag{22}$$

Post-collision properties are then drawn from the deviational distribution

$$\frac{\hbar\omega D(\omega, p)}{4\pi\tau(\omega, p, T)} \left( \frac{1}{\exp\left(\frac{\hbar\omega}{k_{\rm B}\tilde{T}}\right) - 1} - \frac{1}{\exp\left(\frac{\hbar\omega}{k_{\rm B}T_{\rm eq}}\right) - 1} \right). \tag{23}$$

This process provides an opportunity for introducing particle cancellation between positive and negative particles and thus prevents uncontrolled growth of the number of particles in the simulation as a result of particle generation processes, such as boundary conditions, or source terms to be discussed below. The cancellation process takes advantage of the fact that energy conservation only requires the net amount of energy to be conserved during scattering; in other words, positive and negative particles selected for deletion may be cancelled and only the *net* number of particles (of the appropriate sign) needs to be generated. Some boundary conditions (e.g. isothermal boundaries) also contribute to particle cancellation by allowing cancellation of particles incident upon them. More details can be found in [3].

As discussed in Section 2.4, in the limit of small deviation from equilibrium, deviational methods exhibit relative statistical uncertainty that is independent of the deviation from equilibrium. This is verified in Figure 1, which shows the average statistical uncertainty in the heat flux normalized by the heat flux, $\sigma_{\bar{q''}}/\bar{q''}$, as a function of the normalized temperature difference $|T_{\rm l} - T_{\rm r}|/T_{\rm eq}$; note that for the problem considered here, namely heat transfer between two parallel walls at temperatures $T_{\rm l}$ and $T_{\rm r}$ and at a distance apart such that $Kn = 1$, the heat flux is constant across the

[DOI: 10.1299/mer.2014fe0013]

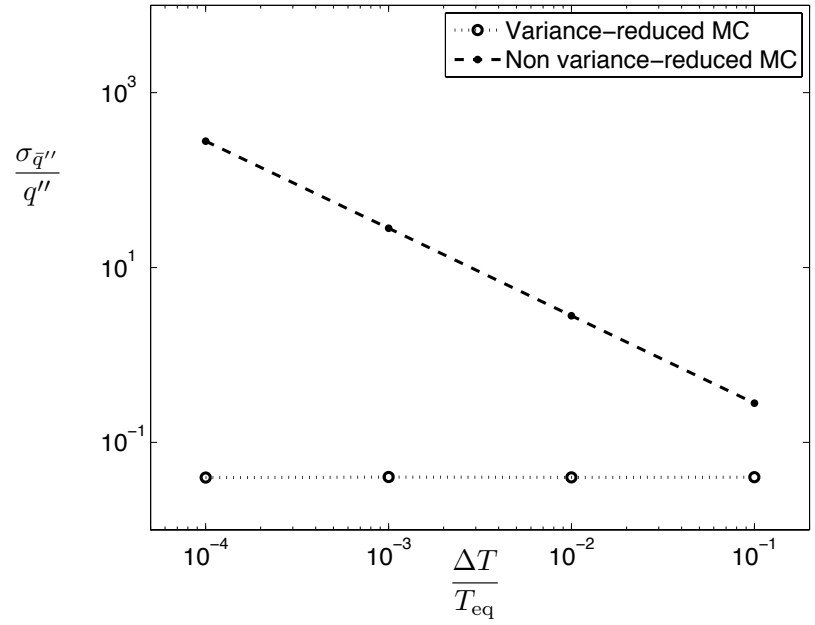


Figure 1: Ratio $\sigma_{\bar{q}''}/q''$ as a function of $\Delta T/T_{\mathrm{eq}}$.

domain. Specifically, the figure compares the statistical uncertainty of the variance-reduced case with $T_{\mathrm{eq}} = 300$ K to the non-variance-reduced case for the silicon model (dispersion relation and relaxation times) described in [50]. The figure verifies that in the variance-reduced case, the standard deviation is proportional to $\Delta T = |T_{\mathrm{l}} - T_{\mathrm{r}}|$. For $\Delta T/T_{\mathrm{eq}} = 0.1$—which, for $T_{\mathrm{eq}} = 300$ K, corresponds to a relatively large amplitude of 30K—the standard deviation is reduced by a factor of 7, meaning that the variance-reduced method can reach a given level of statistical uncertainty using $7^2 \approx 50$ times less samples. For $\Delta T/T_{\mathrm{eq}} = 0.01$, which corresponds to a temperature difference of 3K, the speedup is approximately 5,000 times. This is particularly important because it is achieved without introducing any approximation, using algorithms of complexity that is comparable to traditional (non-variance reduced) MC methods.

## 4. Spatially varying controls

In the case $T_{\mathrm{eq}} = T_{\mathrm{eq}}(\mathbf{x})$, the equation governing the deviation $e^{\mathrm{d}} = e - e^{\mathrm{eq}}_{T_{\mathrm{eq}}(\mathbf{x})}$ can be written as

$$\frac{\partial e^{\mathrm{d}}}{\partial t} + \mathbf{V}_g \cdot \nabla_{\mathbf{x}} e^{\mathrm{d}} = \frac{\left(e^{\mathrm{loc}} - e^{\mathrm{eq}}_{T_{\mathrm{eq}}(\mathbf{x})}\right) - e^{\mathrm{d}}}{\tau(\omega, p, T)} - \mathbf{V}_g \cdot \nabla_{\mathbf{x}} T_{\mathrm{eq}} \frac{de^{\mathrm{eq}}_{T_{\mathrm{eq}}(\mathbf{x})}}{dT}, \tag{24}$$

where the new term on the RHS is a result of the fact that $e^{\mathrm{eq}}_{T_{\mathrm{eq}}}$ is no longer constant. In simulations, this term can be interpreted as a source of *computational* particles. The

[DOI: 10.1299/mer.2014fe0013]

number of particles emitted by this source (per timestep), the distribution of these particles, as well as a discussion of efficient methods for generating these particles from this distribution are discussed in detail in [29]. Here we discuss briefly the rationale for using a spatially variable control.

Although a spatially variable control leads to a moderately more complex algorithm, it provides additional freedom for tailoring the control to the local conditions and thus improving variance reduction. As has been shown in previous work [49, 51], the computational benefit from this approach can be significant [51], particularly in the limit $Kn \to 0$ where the distribution function is described very well [39] by a spatially dependent equilibrium distribution (known as the local equilibrium). In fact, this endows methods employing variable controls with the ability to efficiently simulate multiscale phenomena, since in regions where kinetic effects are not important ($Kn \to 0$), very few particles are used, and the system is primarily described by the deterministic control. In the present paper this is demonstrated again in the context of multiscale simulation, discussed in Section 8.

Source term formulations are also valuable for simulating systems under the action of large-scale temperature gradients. In some cases [3], source terms are useful for reducing the dimensionality of such systems (rather than explicitly simulating this dimension and using boundary conditions to impose a temperature difference and thus a gradient), while in other cases they can be used to efficiently apply temperature gradients in complex geometries, which is of particular interest in the context of calculating the effective thermal conductivity of nanostructured materials [29].

## 5. Efficient methods for linearized problems

Although the deviational formulation introduces no approximation and can therefore be used for arbitrary deviations from equilibrium, computational benefits are obtained when deviations from equilibrium are small. Previous studies have shown [52] that the range over which large computational benefits are observed includes the regime where linearization of the governing equation is valid as well as the early non-linear regime. It is therefore justified to work with the linearized form of the governing equation, especially if further benefits, such as additional simplicity, follow. In the case of the relaxation time approximation, it was recently shown [53] that in addition to simplicity, considering the linearized Boltzmann equation results in considerable computational advantages.

The linearized BTE in the relaxation time approximation can be written as

$$\frac{\partial e^{\mathrm{d}}}{\partial t} + \mathbf{V}_g \cdot \nabla_{\mathbf{x}} e^{\mathrm{d}} = \frac{\mathcal{L}(e^{\mathrm{d}}) - e^{\mathrm{d}}}{\tau(\omega, p, T_{eq})}, \tag{25}$$

where

$$\mathcal{L}(e^{\mathrm{d}})(\omega) = \frac{de^{\mathrm{eq}}_{T_{\mathrm{eq}}}}{dT}(\tilde{T} - T_{\mathrm{eq}}), \tag{26}$$

[DOI: 10.1299/mer.2014fe0013]

where $\tilde{T}$ is the pseudo-temperature defined in (11).

The (linearized) dynamics described by this equation can be simulated by deleting particles with probability (22) and generating particles from the distribution

$$\frac{D}{4\pi\tau(T_{\rm eq})}\frac{de^{\rm eq}_{T_{\rm eq}}}{dT}(\tilde{T}-T_{\rm eq}). \tag{27}$$

The key to additional computational benefits is to realize that once normalized, this distribution does not depend on $(\tilde{T}-T_{\rm eq})$ and thus knowledge of $\tilde{T}$ (other than for reporting purposes) is not necessary. This, however, implies that particle trajectories can be simulated independently (knowledge of $\tilde{T}$ was the only consideration coupling particle trajectories and necessitating a small timestep).

Uncoupled particle trajectories can be integrated significantly more efficiently using algorithms known in the Monte Carlo literature as Kinetic Monte Carlo (KMC) [54]. These algorithms exploit the fact that starting from a scattering event (boundary or relaxation) the particle trajectory will be a straight line until the next scattering event. For a spatially constant $T_{\rm eq}$, the time between phonon-phonon scattering events is exponentially distributed, implying that the time to the next relaxation event can be calculated from $\Delta t = -\tau(\omega,p,T_{\rm eq})\ln(\mathcal{R})$, where $\mathcal{R}$ is a uniformly distributed random number in $(0,1)$. Therefore, integration proceeds by finding and processing the next scattering event, by comparing $\Delta t$ to the time traveled by the particle until it encounters a boundary. The earliest scattering event is processed and the process is repeated until the final time of interest is reached.

The benefits associated with the linearized formulation are numerous: in addition to being significantly easier to code, the linearized simulation is significantly more efficient because it involves less operations per simulated particle and uses significantly less memory. Moreover, because it allows each particle to evolve at its own characteristic time rather than requiring a timestep that is much smaller than the smallest relaxation time, additional computational benefits are enjoyed, especially for problems with disparate relaxation times. Additional benefits are obtained in the case of steady problems, which the linearized method can simulate without the need to explicitly march to the steady state from an initial condition. Steady-state formulations are discussed in [29, 53].

Although typically considerable, the speedup compared to other methods will be problem dependent as it depends on a number of factors. It was reported in [53] that over a number of applications, the speedup ranged between a factor of 100 and 1000. Figure 2 shows the surface temperature as a function of time in a grating experiment (sometimes referred to as Transient ThermoReflectance—see Section 6 for details) simulated with the timestep-based deviational method and with the linearized, KMC-type method. For similar computational times, the latter could calculate the response over significantly longer time scales (around three orders of magnitude).

[DOI: 10.1299/mer.2014fe0013]

## 6. Adjoint formulations

The computational speedup obtained by the linearized KMC-type algorithm described in the previous section is a manifestation of the fact that a linearized governing equation will in general be more amenable to analysis than its non-linear counterpart. In fact, more speedup is possible by exploiting yet another feature stemming from the linearity of the operators involved, namely the duality between the linearized Boltzmann equation and its adjoint, using techniques already developed in the fields of neutron and photon transport, and more generally in linear transport theory [55,56]. The methods described below are particularly useful in problems where the quantity of interest is the result of integration over a small region of (phase) space. For such problems, the number of particle trajectories contributing to the averaging process is small, leading to high statistical uncertainty. Adjoint methods offer the option to replace the integration domain with its adjoint; if the latter is significantly larger and thus more likely to be visited by particles, considerable computational gains can be realized. The basic principles behind such formulations are reviewed below.

### 6.1 The adjoint Boltzmann equation

The adjoint formulation is most conveniently presented in general form using the concept of sources and detectors [55]. Sources are responsible for particle generation and can be used to represent boundary conditions, initial conditions as well as sources of particles due to a spatially variable equilibrium introduced in Section 4. In what follows, we will use the notation $q$ for the sum of all sources in a given problem [57], such that energy-based deviational particles are emitted from $(4\pi)^{-1}D(de^{\mathrm{eq}}/dT)q$. The Boltzmann transport equation with such a source term reads

$$\frac{\partial \psi}{\partial t} + \mathbf{V}_g \cdot \nabla_{\mathbf{x}} \psi = \frac{\mathcal{L}(\psi) - \psi}{\tau} + q, \tag{28}$$

where $\psi = e(de^{\mathrm{eq}}/dT)^{-1}$ and

$$\mathcal{L}(\psi) = \frac{\int \frac{D}{4\pi\tau}\frac{de^{\mathrm{eq}}}{dT}\psi d\omega d^2\mathbf{\Omega}}{\int \frac{D}{\tau}\frac{de^{\mathrm{eq}}}{dT}d\omega}. \tag{29}$$

Detectors are generalizations of the sampling process used to extract macroscopic quantities of interest, such as the average temperature in a given volume at a given time. Mathematically, a detector is represented by a characteristic function $h$ related to the quantity of interest $\mathcal{I}$ by

$$\mathcal{I} = \int h\frac{D}{4\pi}e^{\mathrm{d}}d\omega d^2\mathbf{\Omega}d^3\mathbf{x}dt = \int h\frac{D}{4\pi}\frac{de^{\mathrm{eq}}}{dT}\psi d\omega d^2\mathbf{\Omega}d^3\mathbf{x}dt, \tag{30}$$

where the integration spans the phase space and time; here, the sum over phonon polarizations is implied. The function $h$ contains information not only on the type of

[DOI: 10.1299/mer.2014fe0013]

quantity that is extracted (temperature, heat flux, ...) but also on the location over which the quantity is averaged. For instance, the detector associated with the average deviational temperature within a volume $V$ and between $t_1$ and $t_2$ is

$$h = \frac{1}{CV(t_2 - t_1)} \mathbb{1}_V \mathbb{1}_{[t_1,t_2]}, \tag{31}$$

where $C$ refers to the heat capacity of the materials of consideration and $\mathbb{1}_V$ refers to the function which takes the value 1 inside the volume $V$ and 0 otherwise. For the temperature at a given time $t_0$, this quantity would instead be

$$h = \frac{1}{CV} \mathbb{1}_V \delta(t - t_0), \tag{32}$$

where $\delta(t - t_0)$ refers to the Dirac delta function centered in time on $t_0$.

Now consider the adjoint Boltzmann equation

$$-\frac{\partial \psi^*}{\partial t} - \mathbf{V}_g \cdot \nabla_{\mathbf{x}} \psi^* = \frac{\mathcal{L}(\psi^*) - \psi^*}{\tau} + h. \tag{33}$$

Particles simulating the adjoint solution $\psi^*$ evolve backwards in time and are emitted by the adjoint source that is, in fact, $h$, or in other words, the detector in the original problem. Let us also introduce the adjoint quantity of interest $\mathcal{I}^*$ which uses the source $q$ as a detector. Using integration by parts and the above definitions, one can show that

$$\begin{aligned}
\mathcal{I}^* &= \int q \frac{D}{4\pi} \frac{de^{\mathrm{eq}}}{dT} \psi^* d^3\mathbf{x} d\omega d^2\mathbf{\Omega} dt && (34)\\
&= \int \left[ \frac{\partial \psi}{\partial t} + \mathbf{V}_g \cdot \nabla_{\mathbf{x}} \psi - \frac{\mathcal{L}(\psi) - \psi}{\tau} \right] \frac{D}{4\pi} \frac{de^{\mathrm{eq}}}{dT} \psi^* d^3\mathbf{x} d\omega d^2\mathbf{\Omega} dt && (35)\\
&= \int \psi \frac{D}{4\pi} \frac{de^{\mathrm{eq}}}{dT} \left[ -\frac{\partial \psi^*}{\partial t} - \mathbf{V}_g \cdot \nabla_{\mathbf{x}} \psi^* - \frac{\mathcal{L}(\psi^*) - \psi^*}{\tau} \right] d^3\mathbf{x} d\omega d^2\mathbf{\Omega} dt && (36)\\
&= \int \psi \frac{D}{4\pi} \frac{de^{\mathrm{eq}}}{dT} h d^3\mathbf{x} d\omega d^2\mathbf{\Omega} dt = \mathcal{I} && (37)
\end{aligned}$$

which suggests that solving the adjoint problem with source $h$ and a detector that is identical to the source of the original problem ($q$) is equivalent in terms of final answer to solving the original (forward) problem (with source $q$ and detector $h$). In the derivation above, expression (36) was obtained from (35) by integration by parts, where surface terms proportional to $\psi\psi^*$ evaluated at the phase space boundaries were assumed to go to zero. This is usually the case for problems that can be simulated by the deviational Monte Carlo method [55] and is made possible by the inclusion of the boundary and initial conditions in the source term which allows the extension of the domain of integration beyond those boundaries.

The above property ($\mathcal{I}^* = \mathcal{I}$) can be used to alleviate the computational limitations arising from problems in which the detector, $h$, is small, such as, for example, when the temperature in a small region of space (e.g. a point) is required. The adjoint formulation

[DOI: 10.1299/mer.2014fe0013]

uses $h$ as a source and $q$ as a detector; if $q$ extends over a large region of space, replacing $h$ by $q$ (and solving the adjoint problem) brings considerable improvement.

One example application is the simulation of the Transient ThermoReflectance (TTR) experiment which has received significant interest recently [18, 58]; KMC-type Monte Carlo simulations have already been employed for the simulation of this problem [53, 59] bringing computational savings compared to traditional MC methods and timestep based deviational methods. In this problem, a thin material layer resting on a silicon substrate is heated using a short laser pulse at time $t = 0$. It is usually assumed that the initial deviational temperature field induced by the laser pulse is of the form

$$T_i(\mathbf{x}) = T_1 \exp(-\beta z - \frac{r^2}{2R_0^2}), \tag{38}$$

where $z$ and $r$ represent the depth and the distance from the center of the heated zone, respectively. The values of $T_1$, the penetration depth $\beta^{-1}$ and the characteristic radius $R_0$ depend on the physical characteristics of the laser used. The resulting evolution of the temperature field is unknown and needs to be solved using the BTE because the material layer size is on the order of the phonon mean free path and the problem characteristic evolution time is on the order of the mean time between scattering events.

Connection to experiments is made by measuring the surface temperature evolution for $t > 0$; in the "forward" Monte Carlo method, the probability for a particle to be exactly located at the surface at a given time is zero. As a result, in previous simulations [3] the surface temperature was *approximately* measured by averaging particle contributions in a layer of finite thickness adjacent to the surface. On the other hand, the adjoint formulation allows a direct measurement of the surface temperature by switching the detector with the source: in this case, the material surface becomes a source of particles distributed over time (since the temperature at the surface was to be detected as a function of time), while the initial temperature distribution, $T_i(\boldsymbol{x})$, which was the initial source of non-equilibrium, becomes the detector and records particles which, after being initialized at $t > 0$ are integrated backwards in time and contribute $T_i(\boldsymbol{x}_j(t = 0))/N$ each, where $\boldsymbol{x}_j(t = 0)$ denotes the position of particle $j$ at $t = 0$ (the temperature field can be used as an estimator because the heat capacity, $C$, appears both in the effective energy and the detector and cancels). This formulation replaces the original detector whose volume is zero with a detector whose volume is finite and thus, theoretically provides infinite speedup since the probability of collecting samples goes from zero to a finite number. Practically speaking, as explained above, calculations in the forward case collect samples by approximating the surface as a volume of small thickness. Figure 2 shows the results obtained from such a simulation with the results obtained by an adjoint calculation for the temperature at one point. The forward calculation averages the temperature over a cylinder of radius $10\mu$m and thickness 5nm. As can be seen from the figure, this approximate approach achieves comparable variance that comes at the expense of some error due to averaging over a finite region of space.

We also note that adjoint formulations are sufficiently general and do not require a particular numerical implementation (i.e. timestep based, or KMC-type). The adjoint

[DOI: 10.1299/mer.2014fe0013]

results in figure 2 were obtained using the KMC-type method of Section 5.

The adjoint method has already proven useful in [60] where it is used as a means of calculating the contributions of each phonon frequency mode to heat conduction in nanocrystalline materials (namely, silicon and silicon-germanium). For such calculations, the "forward" method performs poorly in resolving the contributions of low frequency phonons: the latter usually feature a low density of states and thus the occurrence of a particle contributing to the corresponding estimate is rare, resulting in a large statistical uncertainty. In other words, the forward Monte Carlo technique tends to under-resolve the contribution of low-frequency phonons and to over-resolve the contribution of high-frequency phonons. The "adjoint" technique alleviates this stiffness in a simple and elegant manner. Regardless of the phonon mode, it guarantees that each computational particle contributes to the calculated estimate. Using this technique, Hua and Minnich have shown that low frequency phonons still significantly contribute to the thermal conductivity in spite of the small grain size.

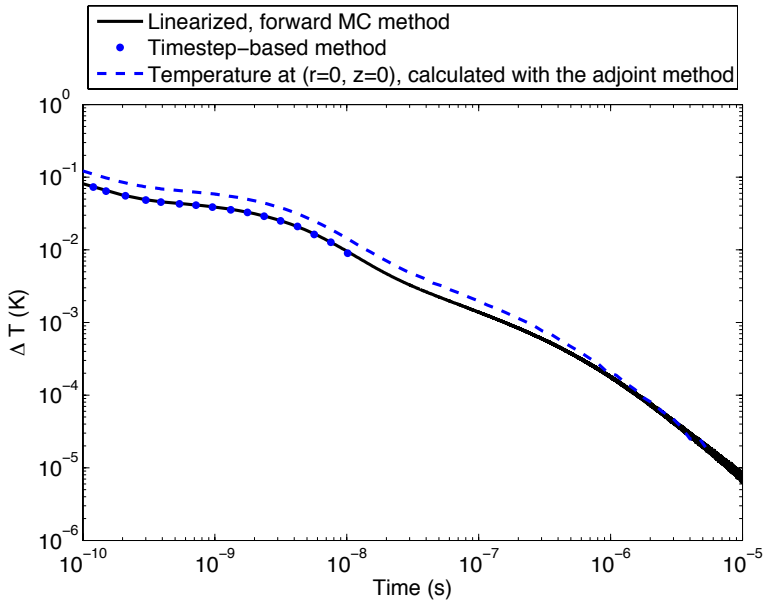


Figure 2: Temperature at point $(r = 0, z = 0)$ from an adjoint solution as a function of time, compared to the forward solution averaged over a finite region of space. The latter is obtained using both a timestep-based and a KMC-type method. In these calculations, the following model parameters were used: $T_1 = 1\text{K}$, $\beta^{-1} = 7\text{nm}$ and $R_0 = 15\mu m$.

## 7. Simulation of the ab initio collision operator

The advent of two-dimensional materials, for which the relaxation-time approximation predicts a divergent thermal conductivity with material size, has served to highlight

[DOI: 10.1299/mer.2014fe0013]

the limitations of the relaxation-time approximation and show that some of its success was a result of fortuitous cancellation of errors [61]; for example, perhaps as a result of neglecting coupling between out of equilibrium modes, this model fails to capture the distribution of thermal energy transport across modes [20, 21, 62].

Until recently, methods for solving the Boltzmann equation with the ab initio scattering operator (2) have been limited to solutions of the space-homogeneous, time-independent problem associated with determining the thermal conductivity of (homogeneous) semiconductors [20, 21, 34, 62, 63]. Previous studies used iterative methods to solve the homogeneous linearized Boltzmann equation. These solutions have been limited to zero spatial dimensions due to two reasons: first, the large computational cost associated with evaluation of the scattering operator—in addition to identifying all the possible pathways associated with a particular scattering process ($\mathbf{k} \to \mathbf{k}' + \mathbf{k}''$ or $\mathbf{k} + \mathbf{k}' \to \mathbf{k}''$) and calculating the matrix elements associated with the Hamiltonian of interaction (e.g. $\mathcal{Q}_{\mathbf{k}p}^{\mathbf{k}'p',\mathbf{k}''p''}$ of (2))—makes formulations requiring frequent evaluation of this operator intractable; second, because the functional form of this operator differs significantly from traditional operators for which direct or deviational Monte Carlo procedures have been developed—for example, it involves three-phonon processes instead of the "four" molecule processes involved in the hard-sphere operator and its variants [64]—procedures for efficiently sampling these scattering events, up until recently, had not been developed.

Recently, a deviational simulation method was developed [65–67] for simulating the Boltzmann equation using the ab initio scattering operator. This method writes the Boltzmann equation in the form

$$\frac{\partial e_i^{\mathrm{d}}}{\partial t} + [\mathbf{V}_g]_i \cdot \nabla_{\mathbf{x}} e_i^{\mathrm{d}} + [\mathbf{V}_g]_i \cdot \nabla_{\mathbf{x}} e_i^{\mathrm{eq}} = \sum_j B_{ij} e_j^{\mathrm{d}}, \tag{39}$$

where $[\mathbf{V}_g]_i$ denotes the group velocity of state $i$ and the matrix $\mathbf{B}$ represents the action of the linearized scattering operator on $e_j^{\mathrm{d}}$; the latter denotes the *discrete in reciprocal (wavevector) space* energy distribution, namely $e_j^{\mathrm{d}} = e^{\mathrm{d}}(\mathbf{x}, \mathbf{k}_j, t)$, where $\mathbf{k}_j$, $j = 1, ..., N_{\mathrm{states}}$ denotes the discrete states in which the reciprocal space is discretized. The latter is necessary due to a lack of a computationally tractable continuous model—the interaction terms are typically calculated on a discrete grid and tabulated for later use, because their real time calculation is overwhelmingly expensive.

Simulation of (39) via deviational procedures requires small modifications due to the discrete nature of the distribution in reciprocal space. It also requires an algorithm for simulating the effect of the linearized scattering operator, which here is written in the form

$$\left[\frac{df}{dt}\right]_{\mathrm{scatt}} = \sum_j B_{ij} e_j^{\mathrm{d}}. \tag{40}$$

Despite being suggestive of a Markov chain formulation, Markov-chain related simulation processes cannot be used for this problem for two reasons: first, the distribution $e_i^{\mathrm{d}}$

[DOI: 10.1299/mer.2014fe0013]

can take positive or negative values (since it represents a deviational quantity); second, the elements of the propagator,

$$\boldsymbol{P}(\Delta t) = e^{\boldsymbol{B}\Delta t} = \sum_{k=0}^{\infty} \frac{\Delta t^k}{k!} \boldsymbol{B}^k, \tag{41}$$

can be negative (a consequence of having negative off-diagonal elements in $\mathbf{B}$ due to three phonon coupling). The algorithm developed in [65–67] for integrating (40) is exact in time (no timestep error) and is strictly energy conserving, but requires particle cancellation because it results in the generation of additional particles. Although particle cancellation occurs at the boundaries (see Section 3), when the scattering operator creates additional particles, boundaries typically do not provide sufficient cancellation in the scattering-dominated limit ($Kn < 1$) [68]. In the case discussed here, particle cancellation can be effected relatively efficiently, but results in discretization error since cancelled particles will not be at exactly the same physical location (particle states in reciprocal space are discrete and therefore particles in the same wavevector state but of opposite sign can be deleted). This places a rather strict requirement on the size of cancellation cells, which are, in this algorithm, the only contribution to spatial discretization. In other words, the development of more accurate (higher-order) methods for treating particle cancellation, or alternatively, new algorithms that do not require cancellation would constitute an important improvement to this field.

We also note that one advantage of Monte Carlo methods, as opposed to deterministic approaches, is that there is no underlying need for discretizing the reciprocal space. In [65–67], reciprocal space discretization was unavoidable because no acceptable continuous description of the scattering operator in reciprocal space was available. If such a representation is developed, either for the linearized operator used in this work or its non-linear counterpart (Eq. (2)), it could lead to more efficient Monte Carlo algorithms and be particularly useful for three dimensional problems.

## 8. Multiscale problems via algebraic decomposition

Efficient simulation of multiscale problems has received considerable attention in the context of a wide range of applications including kinetic transport. As discussed in more detail in [49], deviational methods exhibit a number of features that makes them very well suited for the simulation of multiscale problems. Specifically, by separating out the equilibrium component of the distribution function, computational resources are focused on the regions where the deviation from equilibrium is appreciable. This is, in essence, the objective of multiscale methods; namely, the ability to reserve the use of the expensive, high-fidelity, computational descriptions only in regions where they are needed, while using an inexpensive description where possible. In contrast to traditional approaches [69, 70] which achieve this goal using domain decomposition (of the solution domain), deviational methods achieve this using **algebraic decomposition** (of the distribution function). This approach ensures that computational resources are focused

[DOI: 10.1299/mer.2014fe0013]

on regions of high non-equilibrium which are, primarily, the regions where the traditional continuum description fails. Moreover, this decomposition occurs *automatically and adaptively* with no user intervention and without requiring any simplifying assumptions or approximate coupling techniques.

An example of the computational benefits of algebraic decomposition is the simulation of the TTR experiment discussed in Section 6: due to the localized nature of the heating, large parts of the computational domain remain in equilibrium. At early times, in particular, only a very small region of space is under non-equilibrium conditions while the remainder of the domain is at equilibrium at the initial domain temperature. Algebraic decomposition uses this information to minimize the number of computational particles required, or alternatively, for a given number of computational particles, resolve the deviation from equilibrium more effectively. The computational savings compared to traditional MC methods are very large [3], both due to variance reduction, but also because the simulation domain does not need to be filled with particles representing the equilibrium distribution in the vast majority of the domain.

The TTR experiment discussed above is a special case where equilibrium coincides with the exact continuum solution. In general, regions in which a continuum description is still adequate will exhibit temperature gradients that may be described by Fourier's law. Progress towards taking those gradients into account can be achieved by using a spatially variable (local) equilibrium distribution: it is well known [14, 29] that local equilibrium corresponds to the leading order term in the expansion

$$e = e^{\mathrm{loc}} + Kn\, e_1 + Kn^2\, e_2 + \ldots \quad , \tag{42}$$

which may be used to construct a solution to the BTE in the presence of a homogeneous temperature gradient. The above equation shows that using $e^{\mathrm{loc}}$ as the control ensures that the remainder to be simulated using particles scales as $\mathrm{O}(Kn)$ or higher, ensuring that it goes to zero as characteristic lengthscales become large ($Kn \to 0$). One manifestation of this property is that, in contrast to standard particle simulation methods which become increasingly more expensive as the NSF ($Kn \to 0$) limit is approached (larger length scales imply not only more simulation particles, but also longer evolution timescales), deviational methods with a spatially variable equilibrium distribution become more efficient as this limit is approached, because they are able to relegate increasingly more of the description to the equilibrium part, thus **reducing** the number of particles required for the simulation [49].

Methods with variable equilibrium distributions have been developed for dilute gases [2, 51] and shown to exhibit improved variance reduction, particularly as $Kn \to 0$, as expected. In these formulations, the variable control was implemented as piecewise constant within each cell, requiring source terms resulting from the discontinuities in the control at cell boundaries and making multidimensional implementations complex [49,51]. Using a continuously variable control, which results in a volumetric source term, requires knowledge of the local temperature field as a continuous function of space which is difficult to retrieve from the simulation.

[DOI: 10.1299/mer.2014fe0013]

An alternative approach that sidesteps this issue is to use an asymptotic expansion based on the equilibrium distribution $e^{\mathrm{eq}}_{T_0(\mathbf{x}')}$, namely

$$e = e^{\mathrm{eq}}_{T_0(\mathbf{x}')} + Kn\hat{e}_1 + Kn^2\hat{e}_2 + \ldots \quad , \tag{43}$$

where $T_0(\mathbf{x}')$ is the solution of the heat conduction equation for the temperature field based on no-jump boundary conditions and $\mathbf{x}'$ is the dimensionless space coordinate. Solving the BTE via an asymptotic solution procedure [71–73] can be used to show that

$$\hat{e}_1 = e^{\mathrm{eq}}_{T_1(\mathbf{x}')} + e_{K1}(\mathbf{x}') - \boldsymbol{\Omega}\cdot\nabla_{\mathbf{x}'}e^{\mathrm{eq}}_{T_0(\mathbf{x}')}, \tag{44}$$

where $T_1(\mathbf{x}')$ corresponds to solution of the heat conduction equation subject to jump boundary conditions (see [71–73] for details) and where $e_{K1}(\mathbf{x}')$ is a boundary layer correction that is important close to the boundaries. To minimize complexity, one may instead use the distribution $e^{\mathrm{eq}}_{T_0} - \tau\boldsymbol{V}_g\cdot\nabla_{\mathbf{x}}e^{\mathrm{eq}}_{T_0}$ as a control (written here in dimensional units), which does not require knowledge of the *local* temperature field nor the kinetic boundary layer $e_{K1}$ or the temperature field $T_1$. One complication arising from this formulation is that the source term from which particles need to be generated is

$$q = -\mathbf{V}_g\cdot\nabla_{\mathbf{x}}\left(-\tau\mathbf{V}_g\cdot\nabla_{\mathbf{x}}e^{\mathrm{eq}}_{T_0}\right) = \tau V_g^2\Omega_i\Omega_j\frac{\partial^2 e^{\mathrm{eq}}_{T_0}}{\partial x_i\partial x_j}, \tag{45}$$

where $\Omega_i$ denotes cartesian components of the unit vector $\boldsymbol{\Omega}$. (Note that $\mathcal{L}(e^{\mathrm{eq}}_{T_0} - \tau\boldsymbol{V}_g\cdot\nabla_{\mathbf{x}}e^{\mathrm{eq}}_{T_0}) \neq e^{\mathrm{eq}}_{T_0} - \tau\boldsymbol{V}_g\cdot\nabla_{\mathbf{x}}e^{\mathrm{eq}}_{T_0}$.) Although drawing particles from such a distribution in phase space is theoretically feasible, the routines involved would be delicate to implement in a general way, and represent a significant programming burden. This limitation can be sidestepped by using the adjoint formulation described in Section 6. Specifically, using this source as a detector eliminates the need to generate particles from this distribution and only requires evaluation of integrals of the source term over a particle's trajectory, yielding an algorithm that is considerably simpler.

Figure 3 shows a comparison between a traditional deviational adjoint simulation using $e^{\mathrm{eq}}_{T_{\mathrm{eq}}}$ as a control ($T_{\mathrm{eq}}$ constant) and a simulation using $e^{\mathrm{eq}}_{T_0} - \tau\boldsymbol{V}_g\cdot\nabla_{\mathbf{x}}e^{\mathrm{eq}}_{T_0}$ as a control. All simulations were performed with the same number of particles. More specifically, the figure shows the standard deviation in the temperature field as a function of $Kn$ in a one-dimensional problem of heat transport between two boundaries at different prescribed temperatures; the standard deviation is averaged over local values at fifty equispaced points spanning the simulation domain. The figure shows that the standard deviation observed when using $e^{\mathrm{eq}}_{T_0} - \tau\boldsymbol{V}_g\cdot\nabla_{\mathbf{x}}e^{\mathrm{eq}}_{T_0}$ as a control is proportional to $Kn$. Similar behavior was observed for more complex 2D problems [57]. Therefore, it appears that this formulation exhibits the desirable feature $\sigma(Kn\to 0)\to 0$, which ensures that it is more efficient than a constant-control formulation in the limit $Kn\to 0$. We note that the scaling $\sigma\propto Kn$ observed in figure 3 is superior to the one achieved in [2, 51] ($\sigma\propto\sqrt{Kn}$) using a local equilibrium as a control. The generality of this result, as well as a more general investigation of the statistical uncertainty associated

[DOI: 10.1299/mer.2014fe0013]

with deviational methods and its dependence on physical system properties as well as numerical parameters will be undertaken in the future. We finally note that because MC methods converge with the square root of the number of samples, the speedup is proportional to $\sigma^2$ and is invaluable since as $Kn$ decreases, the computational cost of each particle's trajectory increases. More details can be found in [57].

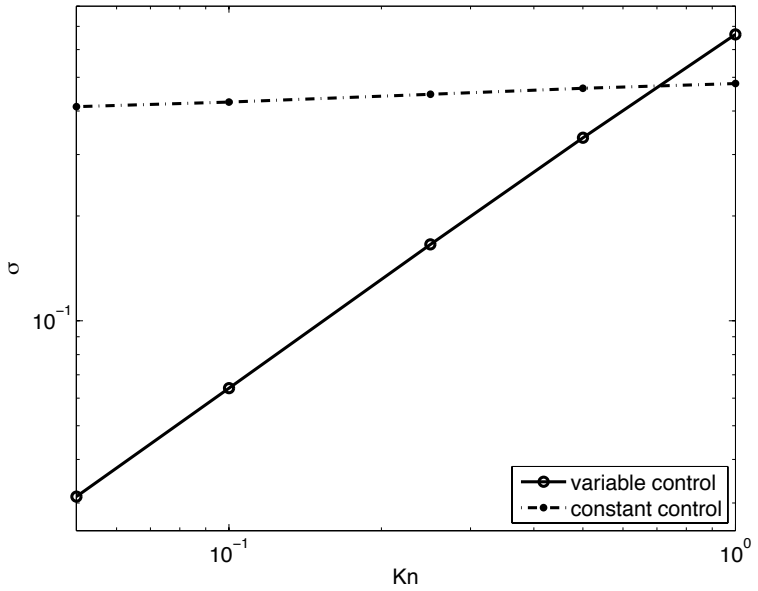


Figure 3: Comparison of the standard deviation $\sigma$ between the adjoint method using a constant equilibrium as a control, and the variable-control method using $e^{\mathrm{eq}}_{T_0} - \tau \boldsymbol{V}_g \cdot \nabla_{\mathbf{x}} e^{\mathrm{eq}}_{T_0}$ as a control. The uncertainty associated with the latter is proportional to $Kn$ and goes to zero as $Kn \to 0$.

## 9. Final remarks

Monte Carlo methods have historically been preferred over deterministic methods for solving the Boltzmann equation because they combine efficiency with simplicity and versatility. Although in some cases deterministic methods can be taylor built to tackle specific (and usually highly idealized) problems more accurately than MC methods (e.g. see [74–76]), such methods typically cannot compete with MC methods over the whole range of problems of interest that includes transient, three-dimensional problems in complex geometries at both high and low $Kn$. One of the most important, but rarely mentioned, advantages of MC methods is their ability to deal with discontinuities in the distribution function naturally and efficiently without numerical instabilities or associated restrictive timesteps, or artificial numerical constructs such as flux limiters. Deviational methods have addressed one of the most important limitations of MC methods, making them generally more efficient but also extending their applicability to even

[DOI: 10.1299/mer.2014fe0013]

more complex problems.

From the developments discussed in this review, two are still in their infancy and present considerable potential for development and computational gains in the future, namely, the simulation of the ab initio collision operator (Section 7) and the adjoint formulation (see Sections 6 and 8). In the case of the ab initio collision operator, we note that the method developed in [65–67] is general and does not rely on assumptions about the material dimensionality. In other words, we expect that deviational simulation methods with ab initio scattering reviewed here should directly extend to 3D materials, making ab initio simulations of all materials of interest possible, provided suitable material information is available (i.e. second and third order force constants for calculation of the scattering matrix $\boldsymbol{B}$). The cost of the method will clearly be larger in three dimensions. The largest computational cost increase is expected to be due to the increase in the number of states in the reciprocal space discretization (each spatial cell requires an independent representation of reciprocal space), but we note that these calculations are already being performed in three dimensions for spatially homogeneous problems [34, 63]. Algorithmic improvements such as the ones, but not limited to those, discussed in Section 7 will go a long way towards making three dimensional simulations using ab initio scattering possible in the near future.

## Acknowledgements

This work was supported in part by the Singapore-MIT Alliance program. J.-P. M. Péraud additionally acknowledges financial support from Ecole National des Ponts et Chaussées, from the Department of Materials Science and Engineering at MIT through a Graduate Fellowship, and from the Total MIT Energy Initiative Fellowship. C. D. Landon acknowledges financial support from the National Science Foundation Graduate Research Fellowship Program and the National Defense Science and Engineering Graduate fellowship.

## References

[1] L. L. Baker and N. G. Hadjiconstantinou. Variance reduction for Monte Carlo solutions of the Boltzmann equation. *Physics of Fluids*, 17:051703, 2005.

[2] T. M. M. Homolle and N. G. Hadjiconstantinou. A low-variance deviational simulation Monte Carlo for the Boltzmann equation. *Journal of Computational Physics*, 226:2341–2358, 2007.

[3] J.-P. M. Péraud and N. G. Hadjiconstantinou. Efficient simulation of multidimensional phonon transport using energy-based variance-reduced Monte Carlo formulations. *Physical Review B*, 84:205331, 2011.

[4] J. M. Hammersley and D. C. Handscomb. *Monte Carlo Methods*. Wiley, New York, NY, 1964.

[DOI: 10.1299/mer.2014fe0013]

[5] N. G. Hadjiconstantinou. The limits of Navier-Stokes theory and kinetic extensions for describing small scale gaseous hydrodynamics. *Physics of Fluids*, 18:111301, 2006.

[6] L. Shi. Thermal transport measurement techniques for nanowires and nanotubes. In *Annual Review of Heat Transfer*, volume 16. Begell House, 2013.

[7] T. Klitsner, J. E. VanCleve, H. E. Fisher, and R. O. Pohl. Phonon radiative heat transfer and surface scattering. *Physical Review B*, 38:7576–7594, 1988.

[8] D. Lacroix, K. Joulain, D. Terris, and D. Lemonnier. Monte Carlo modeling of phonon transport in nanodevices. *Journal of Physics: Conference Series*, 92:1–4, 2007.

[9] A. L. Moore, S. K. Saha, R. S. Prasher, and L. Shi. Phonon backscattering and thermal conductivity suppression in sawtooth nanowires. *Applied Physics Letters*, 93:083112, 2008.

[10] N. A. Roberts and D. G. Walker. Computational study of thermal rectification from nanostructured interfaces. *Journal of Heat Transfer*, 133:092401, 2011.

[11] M. S. Jeng, R. Yang, D. Song, and G. Chen. Modeling the thermal conductivity and phonon transport in nanoparticle composites using Monte Carlo simulation. *Journal of Heat Transfer*, 130:042410, 2008.

[12] M.-J. Huang and P.-Y Chuang. An investigation into the lattice thermal conductivity of random nanowire composites. *International Journal of Heat and Mass Transfer*, 55:3704–3712, 2012.

[13] J. Randrianalisoa and D. Baillis. Monte Carlo simulation of cross-plane thermal conductivity of nanostructured porous silicon films. *Journal of Applied Physics*, 103:053502, 2008.

[14] G. Chen. *Nanoscale Energy Transport and Conversion*. Oxford University Press, New York, NY, 2005.

[15] Q. Hao, G. Chen, and M. S. Jeng. Frequency-dependent Monte Carlo simulation of phonon transport in two-dimensional porous silicon with aligned pores. *Journal of Applied Physics*, 106(11):114321, 2009.

[16] W. Tian and R. Yang. Thermal conductivity modeling of compacted nanowire composites. *Journal of Applied Physics*, 101:054320, 2007.

[17] A. J. Minnich, G. Chen, S. Mansoor, and B. S. Yilbas. Quasiballistic heat transfer studied using the frequency-dependent Boltzmann transport equation. *Physical Review B*, 84(23):235207, 2011.

[18] A. J. Minnich. Determining phonon mean free paths from observation of quasiballistic thermal transport. *Physical Review Letters*, 109:205901, 2012.

[19] A. J. Minnich. Measuring phonon mean free paths using thermal conductivity spectroscopy. In *Annual Review of Heat Transfer*, volume 16. Begell House, 2013.

[20] J. H. Seol, I. Jo, A. L. Moore, L. Lindsay, Z. H. Aitken, M. T. Pettes, X. Li, Z. Yao, R. Huang, D. Broido, N. Mingo, R. S. Ruoff, and L. Shi. Two-dimensional phonon transport in supported graphene. *Science*, 328:213–216, 2010.

[21] L. Lindsay, D. A. Broido, and N. Mingo. Flexural phonons and thermal transport in graphene. *Physical Review B*, 82:115427, 2010.

[DOI: 10.1299/mer.2014fe0013]

[22] A. A. Balandin. Thermal properties of graphene and nanostructured carbon materials. *Nature Materials*, 10:569–581, 2011.

[23] E. Pop, R. W. Dutton, and K. E. Goodson. Analytic band Monte Carlo model for electron transport in Si including acoustic and optical phonon dispersion. *Journal of Applied Physics*, 96:4998, 2004.

[24] D. G. Walker and R. A. Weller. Phonon production and nonequilibrium transport from ion strikes. *IEEE Transactions on Nuclear Science*, 51(6):3318–3321, 2004.

[25] B. T. Wong and M. P. Mengüc. A unified Monte Carlo treatment of the transport of electromagnetic energy, electrons, and phonons in absorbing and scattering media. *J. Quantitative Spectroscopy & Radiative Transfer*, 111:399–419, 2010.

[26] B. T. Wong, M. Francoeur, and M. P. Mengüc. A Monte Carlo simulation for phonon transport within silicon structures at nanoscales with heat generation. *International Journal of Heat and Mass Transfer*, 54:1825–1838, 2011.

[27] E. B. Ramayya, L. N. Maurer, A. H. Davoody, and I. Knezevic. Thermoelectric properties of ultrathin silicon nanowires. *Physical Review B*, 86:115328, 2012.

[28] E. Pop. Monte Carlo transport and heat generation in semiconductors. In *Annual Review of Heat Transfer*, volume 17. Begell House, 2014.

[29] J.-P. M. Péraud, C. D. Landon, and N. G. Hadjiconstantinou. Monte Carlo methods for solving the Boltzmann transport equation. In *Annual Review of Heat Transfer*, volume 17. Begell House, 2014.

[30] E. S. Piekos, S. Graham, and C. C. Wong. Multiscale thermal transport. Technical Report SAND2004-0531, Sandia National Laboratories, 2004.

[31] G. Chen. Size and interface effects on thermal conductivity of superlattices and periodic thin-film structures. *Journal of Heat Transfer*, 119:220–229, 1997.

[32] P. K. Schelling and S. R. Phillpot. Multiscale simulation of phonon transport in superlattices. *Journal of Applied Physics*, 93(9):5377–5387, 2003.

[33] G. P. Srivastava. *The Physics of Phonons*. Taylor & Francis Group, New York, NY, 1990.

[34] J. A. Pascual-Gutiérrez, J. Y. Murthy, and R. Viskanta. Thermal conductivity and phonon transport properties of silicon using perturbation theory and the environment-dependent interatomic potential. *Journal of Applied Physics*, 106:063532, 2009.

[35] D. J. Ecsedy and P. G. Klemens. Thermal resistivity of dielectric crystals due to four-phonon processes and optical modes. *Physical Review B*, 15:59575962, 1976.

[36] J. M. Ziman. *Electrons and Phonons*. Clarendon Press, Oxford, UK, 1960.

[37] J. Y. Murthy. Review of multiscale simulation in sub micron heat transfer. *International Journal of Multiscale Computational Engineering*, 3(1):5–31, 2005.

[38] J. Y. Murthy. In *Annual Review of Heat Transfer*, volume 17. Begell House, 2014.

[39] C. Cercignani. *The Boltzmann Equation and its Applications*. Springer-Verlag, New York, NY, 1988.

[DOI: 10.1299/mer.2014fe0013]

[40] D. G. Cahill, W. K. Ford, K. E. Goodson, G. D. Mahan, A. Majumdar, H. J. Maris, R. Merlin, and S. R. Phillpot. Nanoscale thermal transport. *Journal of Applied Physics*, 93:793–818, 2003.

[41] G. A. Bird. Approach to translational equilibrium in a rigid sphere gas. *Physics of Fluids*, 6:1518–1520, 1963.

[42] F. J. Alexander, A. L. Garcia, and B. J. Alder. Cell size dependence of transport coefficients in stochastic particle algorithms. *Physics of Fluids*, 10:1540–1542, 1998.

[43] F. J. Alexander and A. L. Garcia. The direct simulation Monte Carlo method. *Computers in Physics*, 11:588–593, 1997.

[44] W. Wagner. A convergence proof for Bird's direct simulation Monte Carlo method for the Boltzmann equation. *Journal of Statistical Physics*, 66:1011–1044, 1992.

[45] N. G. Hadjiconstantinou. Analysis of discretization in the direct simulation Monte Carlo. *Physics of Fluids*, 12:2634–2638, 2000.

[46] D. J. Rader, M. A. Gallis, J. R. Torczynski, and W. Wagner. Direct simulation Monte Carlo convergence behavior of the hard-sphere gas thermal conductivity for Fourier heat flow. *Physics of Fluids*, 18:077102, 2006.

[47] K. Aoki, S. Takata, and F. Golse. A rarefied gas flow caused by a discontinuous wall temperature. *Physics of Fluids*, 13:2645–2661, 2001.

[48] N. G. Hadjiconstantinou, A. L. Garcia, M. Z. Bazant, and G. He. Statistical error in particle simulations of hydrodynamic phenomena. *Journal of Computational Physics*, 187:274–297, 2003.

[49] G. A. Radtke, J.-P. M. Péraud, and N. G. Hadjiconstantinou. On efficient simulations of multiscale kinetic transport. *Philosophical Transactions of the Royal Society A*, 371:20120182, 2013.

[50] A. J. Minnich. *Exploring electron and phonon transport at the nanoscale for thermoelectric energy conversion*. PhD thesis, Massachusetts Institute of Technology, Cambridge, MA, 2011.

[51] G. A. Radtke and N. G. Hadjiconstantinou. Variance-reduced particle simulation of the Boltzmann transport equation in the relaxation-time approximation. *Physical Review E*, 79:056711, 2009.

[52] N. G. Hadjiconstantinou, G. A. Radtke, and L. L. Baker. On variance reduced simulations of the Boltzmann transport equation for small-scale heat transfer applications. *Journal of Heat Transfer*, 132:112401, 2010.

[53] J.-P. M. Péraud and N. G. Hadjiconstantinou. An alternative approach to efficient simulation of micro/nanoscale phonon transport. *Applied Physics Letters*, 101:153114, 2012.

[54] A. F. Voter. *Introduction to the Kinetic Monte Carlo Method*, volume 235 of *NATO Science Series*. Springer, 2007.

[55] J. Spanier and E. M. Gelbard. *Monte Carlo Principles and Neutron Transport Problems*. Addison-Wesley, Reading, MA, 1969.

[56] M. F. Modest. Backward Monte Carlo simulations in radiative heat transfer. *Journal of Heat Transfer*, 125:58–62, 2003.

[DOI: 10.1299/mer.2014fe0013]

[57] J.-P. M. Péraud and N. G. Hadjiconstantinou. Adjoint-based deviational Monte Carlo methods for phonon transport calculations. In preparation

[58] A. Schmidt. Pump probe thermoreflectance. In *Annual Review of Heat Transfer*, volume 16. Begell House, 2013.

[59] J.-P. M. Péraud and N. G. Hadjiconstantinou. Deviational phonons and thermal transport at the nanoscale. *The 2012 International Mechanical Engineering Congress and Exposition*, (paper number IMECE2012-87547), 2012.

[60] C. Hua and A. J. Minnich. Importance of frequency-dependent grain boundary scattering in nanocrystalline silicon and silicon-germanium thermoelectrics. *Semiconductor Science Technology*, in press.

[61] D. Singh, J. Y. Murthy, and T. S. Fisher. On the accuracy of classical and long wavelength approximation for phonon transport in graphene. *Journal of Applied Physics*, 110:113510, 2011.

[62] D. Singh, J. Y. Murthy, and T. S. Fisher. Spectral phonon conduction and dominant scattering pathways in graphene. *Journal of Applied Physics*, 110:094312, 2011.

[63] N. Mingo, D. A. Stewart, D. A. Broido, L. Lindsay, and W. Li. Ab initio thermal transport. In *Length-Scale Dependent Phonon Interactions*, pages 137–173. Springer New York, 2014.

[64] G. A. Bird. *Molecular Gas Dynamics and the Direct Simulation of Gas Flows*. Clarendon Press, Oxford, UK, 1994.

[65] C. D. Landon. *A deviational Monte Carlo formulation of ab initio phonon transport and its application to the study of kinetic effects in graphene ribbons*. PhD thesis, Massachusetts Institute of Technology, Cambridge, MA, 2014.

[66] C.D. Landon and N. G. Hadjiconstantinou. Simulation of heat transport in graphene nanoribbons using the ab-initio scattering operator. *The 2014 International Mechanical Engineering Congress and Exposition*, (paper number IMECE2014-36473), in press.

[67] C.D. Landon and N. G. Hadjiconstantinou. Deviational simulation of phonon transport in graphene ribbons with ab initio scattering. *Applied Physics Letters*, submitted.

[68] L. L. Baker and N. G. Hadjiconstantinou. Variance-reduced particle methods for solving the Boltzmann equation. *Journal of Computational and Theoretical Nanoscience*, 5:165–174, 2008.

[69] A. L. Garcia, J. B. Bell, W. Y. Crutchfield, and B. J. Alder. Adaptive mesh and algorithm refinement using direct simulation Monte Carlo. *Journal of Computational Physics*, 154:134–55, 1999.

[70] N. G. Hadjiconstantinou. Hybrid atomistic-continuum formulations and the moving contact-line problem. *Journal of Computational Physics*, 154:245–265, 1999.

[71] J.-P. M. Péraud and N. G. Hadjiconstantinou. On the equations and boundary conditions governing phonon-mediated heat transfer in the small mean free path limit. An asymptotic solution of the Boltzmann equation. *The 2014 International Mechanical Engineering Congress and Exposition*, (paper number IMECE2014-36475), in press.

[72] J.-P. M. Péraud. PhD thesis, Massachusetts Institute of Technology, Cambridge, MA, in progress.

[DOI: 10.1299/mer.2014fe0013]

[73] J.-P. M. Péraud and N. G. Hadjiconstantinou. In preparation.

[74] Y. Sone, T. Ohwada, and K. Aoki. Temperature jump and Knudsen layer in a rarefied gas over a plane wall: Numerical analysis of the linearized Boltzmann equation for hard-sphere molecules. *Physics of Fluids A*, 1(2):363–370, 1989.

[75] Y. Sone, T. Ohwada, and K. Aoki. Numerical analysis of the shear and thermal creep flows of a rarefied gas over a plane wall on the basis of the linearized Boltzmann equation for hard-sphere molecules. *Physics of Fluids A*, 1(9):1588–1599, 1989.

[76] T. Ohwada, Y. Sone, and K. Aoki. Numerical analysis of the Poiseuille and thermal transpiration flows between 2 parallel plates on the basis of the Boltzmann equation for hard-sphere molecules. *Physics of Fluids A*, 1(12):2042–2049, 1989.

[DOI: 10.1299/mer.2014fe0013]